A Temperature-based Controller for a Shape Memory Alloy Actuator

Mohammad H. Elahinia
Assistant Professor
Mechanical Industrial and Manufacturing Engineering Department,
The University of Toledo, Toledo, OH 43606
e-mail: mohammad.elahinia@utoledo.edu

Hashem Ashrafiuon
Professor
Mechanical Engineering Department,
Villanova University, Villanova, Pennsylvania 19085

Mehdi Ahmadian
Professor
Mechanical Engineering Department, Virginia Tech,
Blacksburg, Virginia 24061

Hanghao Tan
Graduate Research Assistant
Mechanical Industrial and Manufacturing Engineering Department, The University of Toledo, Toledo,
OH 43606

This paper presents a robust nonlinear control that uses a state variable estimator for control of a single degree of freedom rotary manipulator actuated by shape memory alloy (SMA) wire. A model for SMA actuated manipulator is presented. The model includes nonlinear dynamics of the manipulator, a constitutive model of the shape memory alloy, and the electrical and heat transfer behavior of SMA wire. The current experimental setup allows for the measurement of only one state variable which is the angular position of the arm. Due to measurement difficulties, the other three state variables, arm angular velocity and SMA wire stress and temperature, cannot be directly measured. A model-based state estimator that works with noisy measurements is presented based on the extended Kalman filter (EKF). This estimator estimates the state vector at each time step and corrects its estimation based on the angular position measurements. The estimator is then used in a nonlinear and robust control algorithm based on variable structure control (VSC). The VSC algorithm is a control gain switching technique based on the arm angular position (and velocity) feedback and EKF estimated SMA wire stress and temperature. Using simulation it is shown that the state vector estimates help reduce or avoid the undesirable and inefficient overshoot problem in SMA one-way actuation control. [DOI: 10.1115/1.1898335]

1 Introduction

Within the significant toolbox of mathematical tools that can be used for stochastic estimation from noisy sensor measurements, one of the most well-known and often-used tools is what is known as the Kalman filter [1,2]. Kalman filter has been extensively used to help control the motion of robotic manipulators [3–7]. However, as far as we know, Kalman filter has not been used to control the motion produced by shape memory alloys (SMAs).

SMAs consist of a group of metallic materials that demonstrate the ability to return to some previously defined shape or size when subjected to the appropriate thermal procedure. The shape memory effect is hysteretic and occurs due to a temperature and stress dependent shift in the material's crystalline structure between two different phases called martensite and austenite which are the low and high temperature phases, respectively. SMA actuators have several advantages for miniaturization such as excellent power to mass ratio, maintainability, reliability, and clean and silent actuation. The disadvantages are low energy efficiency due to conversion of heat to mechanical energy and inaccurate motion control due to hysteresis, nonlinearities, parameter uncertainties, and difficulty in measuring variables such as temperature.

The control research applied to SMAs may be divided into three categories of linear control, pulse width modulation (PWM), and nonlinear control. Different variations of linear proportional integral derivative controls have been explored by some researchers [8,9] while many others have used PWM [10,11]. Several nonlinear control schemes such as fuzzy logic, feedback linearization, and variable structure control (VSC) have also been explored by researchers [12–15].

In this work, we have developed a control algorithm based on VSC. The controller uses an extended Kalman filter (EKF) to estimate the state vector of a single-degree-of-freedom (1-dof) rotary arm. The arm is actuated by a bias type actuator constructed with SMA wire, pulleys, and a linear spring. A nonlinear model is developed based on the arm nonlinear dynamic model, a SMA wire constitutive model, a SMA phase transformation model [16], and a nonlinear heat convection model [13,17]. This model has been experimentally verified in our previous work [13]. An extended Kalman filter is designed for a SMA actuated manipulator and is tested through simulations. The EKF utilizes the control input and the angular position of the arm to predict the other state variables of the system: angular velocity, SMA wire stress, and SMA wire temperature. The incorporation of the stress and temperature estimates into a VSC could help avoid the overshoot problem thus avoiding large delays due to cooling and reheating requirements in SMA one-way actuation.

2 The SMA Arm Model

The single degree-of-freedom (1-dof) SMA-actuated arm is shown in Fig. 1. We have used 150 μm diameter Ni-Ti SMA wire which is actuated by electrical heating. The net actuating torque is the difference between the resulting bias spring and SMA wire torques. The SMA arm model consists of phase transformation, heat transfer, SMA wire constitutive, and arm dynamic blocks. In addition, there is an amplifier, an encoder, and a signal conditioner in the hardware setup.

The nonlinear dynamic model of the arm including spring and payload effects is represented by

$$I_e\ddot{\theta} = \tau_w(\sigma) - \tau_g(\theta) - \tau_s(\theta) - c\dot{\theta}, \tag{1}$$

where τ_w, τ_g, and τ_s are the resulting torques from SMA wire, gravitational loads, and the bias spring, respectively, and σ is the wire stress. I_e is the effective mass moment of inertia of the arm, gripper, and the payload, and c is the torsional damping coefficient approximating the net joint friction.

The SMA wire strain rate $\dot{\varepsilon}$ and joint angular velocity $\dot{\theta}$ are related kinematically as

$$\dot{\varepsilon} = -\frac{2r_p\dot{\theta}}{l_0}, \tag{2}$$

where r_p is pulleys radius and l_0 is the initial length of SMA wire.

Wire constitutive model shows the relationship among stress rate ($\dot{\sigma}$), strain rate, and temperature rate ($\dot{T}$) [18]:

Contributed by the Technical Committee on Vibration and Sound for publication in the JOURNAL OF VIBRATION AND ACOUSTICS. Manuscript received June 10, 2003. Final revision July 7, 2004. Associate Editor: Shirley J. Dyke.

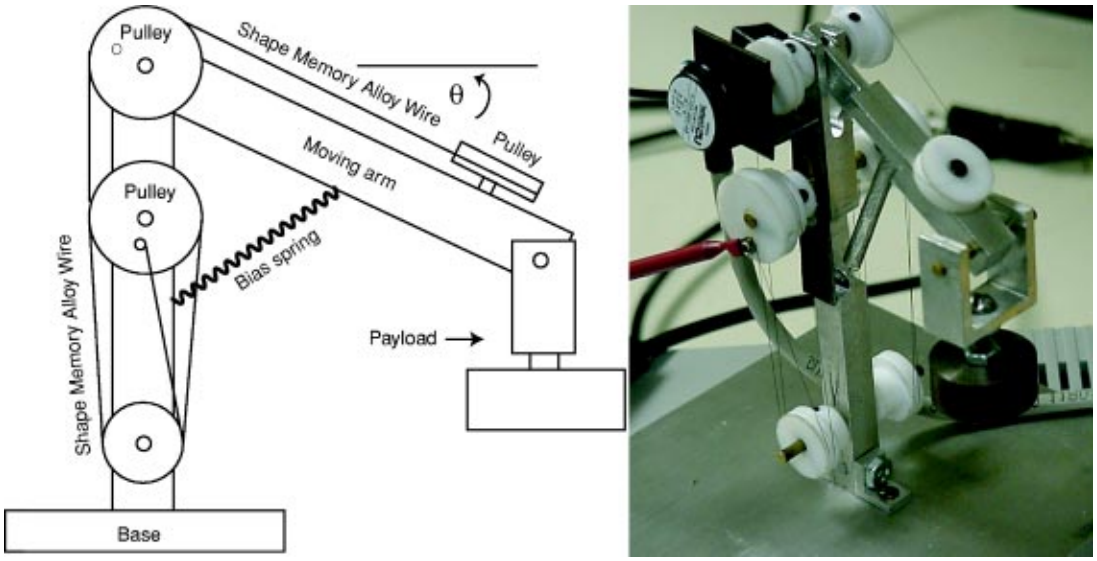

Fig. 1 The 1-dof SMA arm, actuated by NiTi wire and a bias spring

$$\dot{\sigma} = D\dot{\varepsilon} + \theta_T \dot{T} + \Omega\dot{\xi}, \tag{3}$$

where $D=\xi D_M+(1-\xi)D_A$ is the Young modulus, D_A is austenite Young modulus, D_M is martensite Young modulus, θ_T is thermal expansion factor, $\Omega=-D\varepsilon_0$ is phase transformation contribution factor, and ε_0 is the initial (i.e., maximum) strain [16].

Due to hysteretic behavior of SMA wire, the phase transformation equations are different for heating and cooling. Heating results in reverse transformation from martensite to austenite:

$$\xi = \frac{\xi_M}{2}\{\cos[a_A(T-A_s)+b_A\sigma]+1\}, \tag{4}$$

where $0 \leqslant \xi \leqslant 1$ is the martensite fraction coefficient, ξ_M is the maximum martensite fraction obtained during cooling, T is the SMA wire temperature, A_s and A_f are austenite phase start and final temperatures, and $a_A=\pi/(A_f-A_s)$, $b_A=-a_A/C_A$, and C_A are curve fitting parameters.

Cooling results in forward transformation equation from austenite to martensite:

$$\xi = \frac{1-\xi_A}{2}\cos[a_M(T-M_f)+b_M\sigma]+\frac{1+\xi_A}{2}, \tag{5}$$

where ξ_A is the minimum martensite fraction obtained during heating, M_s and M_f are martensite phase start and final temperatures, and $a_M=\pi/(M_s-M_f)$, $b_M=-a_M/C_M$, and C_M are curve fitting parameters.

The SMA wire heat transfer equation consists of electrical heating and natural convection:

$$mc_p\frac{dT}{dt} = \frac{V^2}{R} - hA_c(T-T_\infty), \tag{6}$$

where R is resistance per unit length, c_p is the specific heat, m is mass per unit length and A_c is circumferential area of the SMA wire. Also, V is the applied voltage, T_∞ is the ambient temperature, and h is heat convection coefficient.

3 Extended Kalman Filter

Detailed information on Kalman filter can be found in several references (for example, Ref. [2]). The SMA manipulator model state vector as described in Sec. 2 is defined as

$$x = [\theta\ \dot{\theta}\ \sigma\ T]^T. \tag{7}$$

The discrete model of the system can be derived by approximating the differential equations presented in Sec. 2 to their corresponding backward difference equations. Angular position of the arm at current time may be predicted using previous values of the angular position and velocity as

$$\hat{x}_k^-(1) = \hat{x}_{k-1}(1) + \hat{x}_{k-1}(2)T_s, \tag{8}$$

where T_s is the sampling time. We have used the previous two position samples to predict the arm angular velocity

$$\hat{x}_k^-(2) = \frac{\hat{x}_{k-1}(1)-\hat{x}_{k-2}(1)}{T_s}. \tag{9}$$

Note that the estimated angular velocity is directly related to the measured state variable instead of using Eq. (1) and integrating the angular acceleration. Furthermore, since the SMA wire's stress, is a function of strain, temperature, and phase transformation, Eq. (3) creates an algebraic loop in the model. Hence, the stress is estimated using Eq. (1) instead of the wire constitutive model

$$\hat{x}_k^-(3) = f_3 = [I_e\ddot{\theta} + \tau_g(\hat{x}_{k-1}(1)) + \tau_s(\hat{x}_{k-1}(1)) + c\hat{x}_{k-1}(2)]/(2r_pA_w), \tag{10}$$

where A_w is the SMA wire's cross-sectional area. This way, stress is also directly related to the measured state variable (angular position). The angular acceleration of the arm in Eq. (10) is computed using the difference equation based on the previous two values of the angular velocity

$$\ddot{\theta} = \frac{\hat{x}_{k-1}(2)-\hat{x}_{k-2}(2)}{T_s}. \tag{11}$$

The temperature estimate is merely based on the convection heat transfer equation (6) which depends only on previous temperature value:

$$\hat{x}_k^-(4) = \hat{x}_{k-1}(4) + \frac{V^2/R - hA_c(\hat{x}_{k-1}(4)-T_\infty)}{mc_p}T_s. \tag{12}$$

Note that once the four state variables are estimated, the SMA wire phase transformation index can be directly obtained from Eq.

(4) during reverse transformation (heating) and from Eq. (5) during forward transformation (cooling).

The Jacobian matrix, at each iteration, can be derived using the state equations (8)–(10) and (12),

$$A = \begin{bmatrix} 1 & T_s & 0 & 0 \\ \frac{1}{T_s} & 0 & 0 & 0 \\ A_{31} & c + \frac{1}{T_s} & 0 & 0 \\ 0 & 0 & 0 & A_{44} \end{bmatrix}, \tag{13}$$

where A_{31} and A_{44} are the partial derivatives of state equations (10) and (12) with respect to $x_{k-1}(1)$ and $x_{k-1}(4)$, respectively.

The angular position of the arm is measured. Hence

$$z_k = Hx_k + v_k = [1\ 0\ 0\ 0]x_k + v_k. \tag{14}$$

Here the random variables w_k and v_k represent the process and measurement noise (respectively). They are assumed to be independent (of each other), white, and with normal probability distributions. We use the following initial conditions for the state vector:

$$x_{\text{initial}} = \left[-\frac{\pi}{4}(\text{rad})\ 0(\text{rad/s})\ 98.1(\text{MPa})\ 20(^\circ\text{C}) \right].$$

For the filter, we add uncertainty to the initial condition by selecting $P_0 = I_{4\times4}$ and a relatively small process noise by letting $Q = 1e^{-2}I_{4\times4}$. Initially, we chose a relatively large variance $\sigma_v = 1$ for the measurement noise, assuming that the angular position measurements are corrupted with white noise. Details on the development of the Extended Klaman Filter can be found in our previous work [19].

4 Controller Design

The variable structure control is comprised of two switching surfaces. The main switching condition (surface) is a weighted combination of position and velocity errors,

$$S_1 = \left(\frac{d}{dt} + \lambda \right) \tilde{\theta} = \dot{\tilde{\theta}} + \lambda \tilde{\theta}, \tag{15}$$

where $-\lambda$ is the slope of sliding surface in the phase plane. A boundary layer is introduced around the switching surface S_1, to suppress chattering. Denoting the layer thickness as ϕ_1, the control input is written as

$$\mathbf{u} = \begin{cases} V_{\text{high}} & \text{if } \frac{S_1}{\phi_1} < -1 \\ V_{\text{low}} & \text{if } \frac{S_1}{\phi_1} > +1 \\ KS_1 & \text{if } -1 < \frac{S_1}{\phi_1} < +1, \end{cases} \tag{16}$$

where K is a proportional gain. Generally, increasing the boundary layer thickness, reduces chattering but increases steady-state error. The resulting VSC was implemented and its performance was tested experimentally in our previous study [13].

The reverse phase transformation, which provides upward arm rotation actuation, takes place only when the wire temperature is within the stress-dependent-reverse actuation temperature range (between austenite start, A_{sm}, and final, A_{fm}, temperatures):

$$A_{sm} = A_s + \frac{\sigma}{C_A}, \quad A_{fm} = A_f + \frac{\sigma}{C_A}. \tag{17}$$

In order to avoid overshoot the controller must be able to maintain the SMA wire's temperature between A_{sm} and A_{fm}. Since these transformation temperatures are functions of stress their value decreases as the arm goes beyond the maximum stress position (shown in Fig. 2). To address this issue, a second switching condition is added. This switching condition maintains the temperature of the SMA wire in the actuation range ($A_{sm} < T < A_{\text{fm}}$) while the arm is passing through the maximum stress position. To this end, the control algorithm is the VSC with switching condition of S_1 and when the arm is passing through maximum stress location the controller uses the second switching condition S_2. The second switching condition is introduced in terms of time derivative of the austenite final temperature,

$$S_2 = \frac{dA_{fm}}{dt}. \tag{18}$$

The resulting control algorithm can be written as

$$V = \begin{cases} \mathbf{u} & \text{if } \frac{S_2}{\phi_2} > 1 \\ K_p(T - T_d) & \text{if } -1 < \frac{S_2}{\phi_2} < 1 \\ \mathbf{u} & \text{if } \frac{S_2}{\phi_2} < -1, \end{cases} \tag{19}$$

where T_d is the desired temperature of the SMA wire and ϕ_2 is the thickness of the boundary layer around the switching surface S_2. A linear approximation is used to calculate the desired temperature of the wire. This way, T_d is calculated as a function of desired position and transformation temperatures.

5 Results

The nonlinear SMA model simulations have been previously verified through several experiments [13]. The simulation results with the extended Kalman filter are presented here and compared with the model. In each simulation state variables are collected from simulating the model. Next, the EKF is simulated, which uses the angular position, previously generated from the model. The state vector estimated by the filter is compared with the simulation results of the model.

Figure 3 shows the comparison between the EKF estimated and the nonlinear model state variables for a step input with changing amplitude. Figure 4 represents the estimation performance by the EKF for a sinusoidal input. It can be clearly seen that the filter has an excellent performance for both set-point (step) and tracking (sinusoidal) type tasks. Figure 5 presents the effect of the measurement noise covariances, which is used by the filter to correct its estimates, on the angular position estimation error. Clearly, larger measurement noise causes the filter to reply more on its estimations and lead to larger errors.

In Fig. 6, the performance of the variable structure controller (NVSC) is compared to a controller (PVSC), which is based only on the first switching condition (S_1). The performance of the two controllers are the same for the positions below the maximum stress position. The overshoot problem is reduced with adding the new switching condition, S_2, for the angular positions beyond the maximum stress position. The NVSC prevents the SMA wire from overheating as can be seen in Fig. 7, while the arm passes through the maximum stress position. With the PVSC the wire heats up to the austenite final temperature when the arm reaches the maximum stress position and hence arm has a larger overshoot. Figure 8 presents the effect of the temperature boundary thickness ϕ_T on the overshoot minimization performance of the VSC where the desired angular position is kept constant $\theta_d = 50°$. It can be seen that the overshoot is smaller for the boundary layers with larger thickness. Hence, overshoot can be avoided altogether by increasing the temperature boundary layer.

6 Conclusion

An extended Kalman filter is designed for a rotary SMA actuated manipulator and has been tested through simulations. Satis-

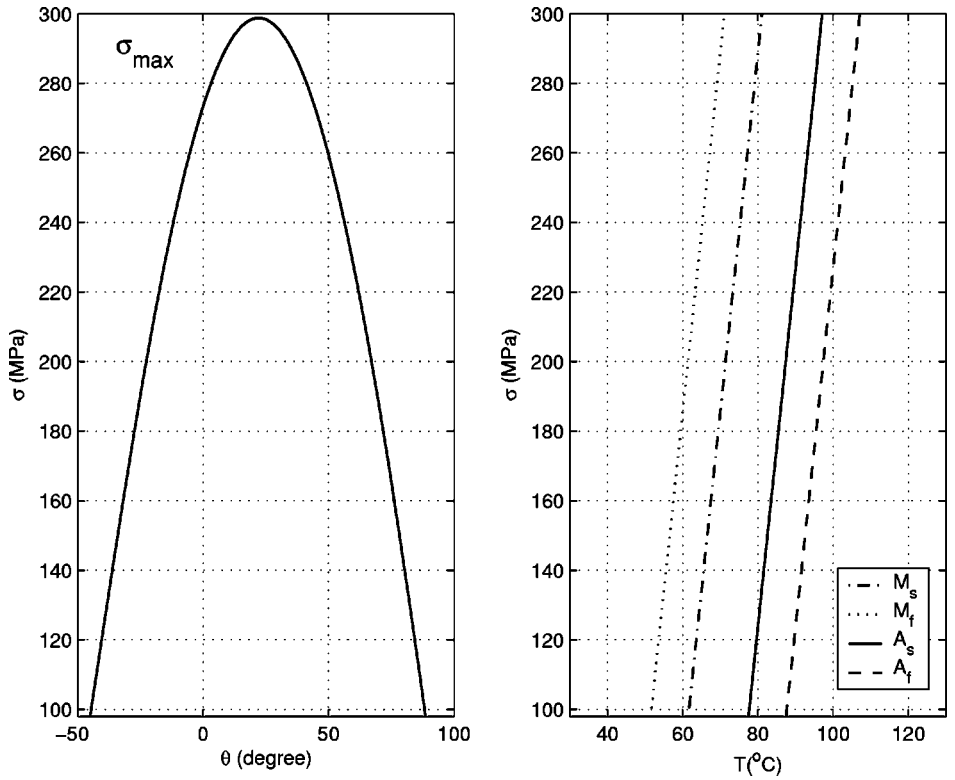

Fig. 2 The stress of the SMA wire reaches a maximum as arm moves upwards; as a result the transformation temperatures also change

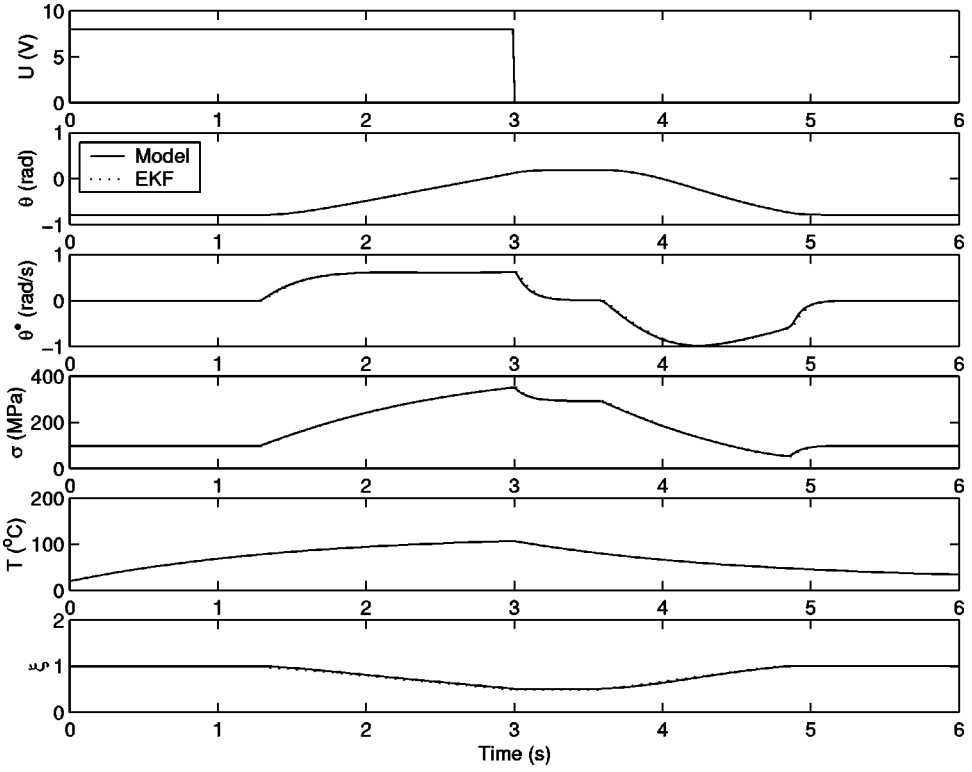

Fig. 3 Comparing the simulation results of the SMA-actuated arm model and the extended Kalman filter for a switching step input

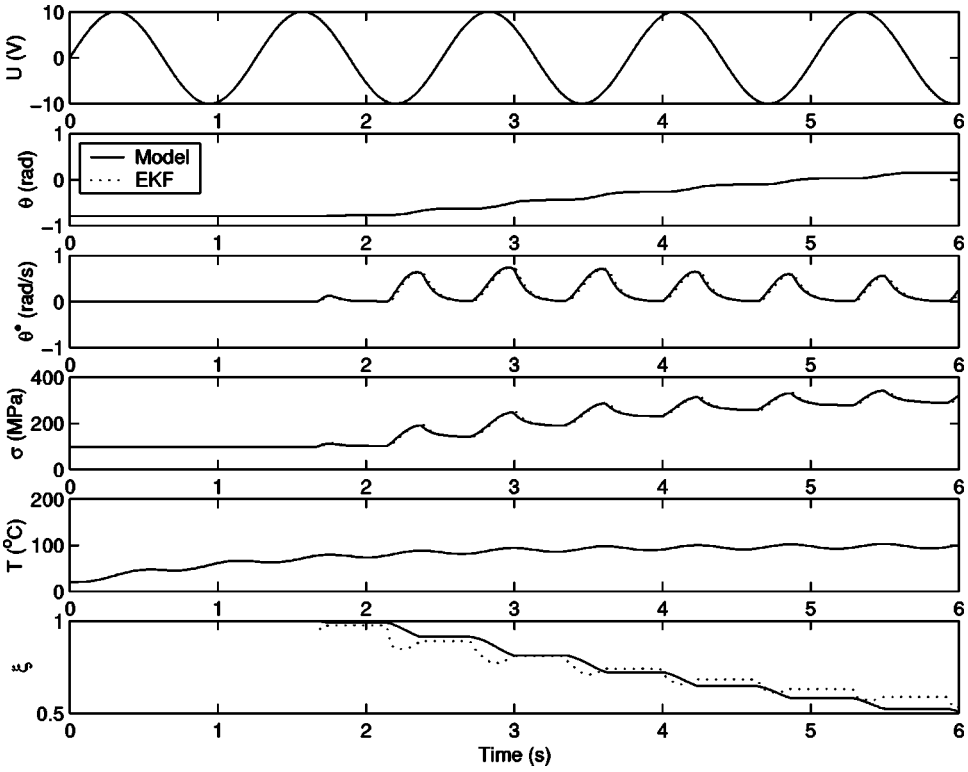

Fig. 4 Comparing the simulation results of the SMA-actuated arm model and the extended Kalman filter for a sinusoidal input (w=5 rad/s)

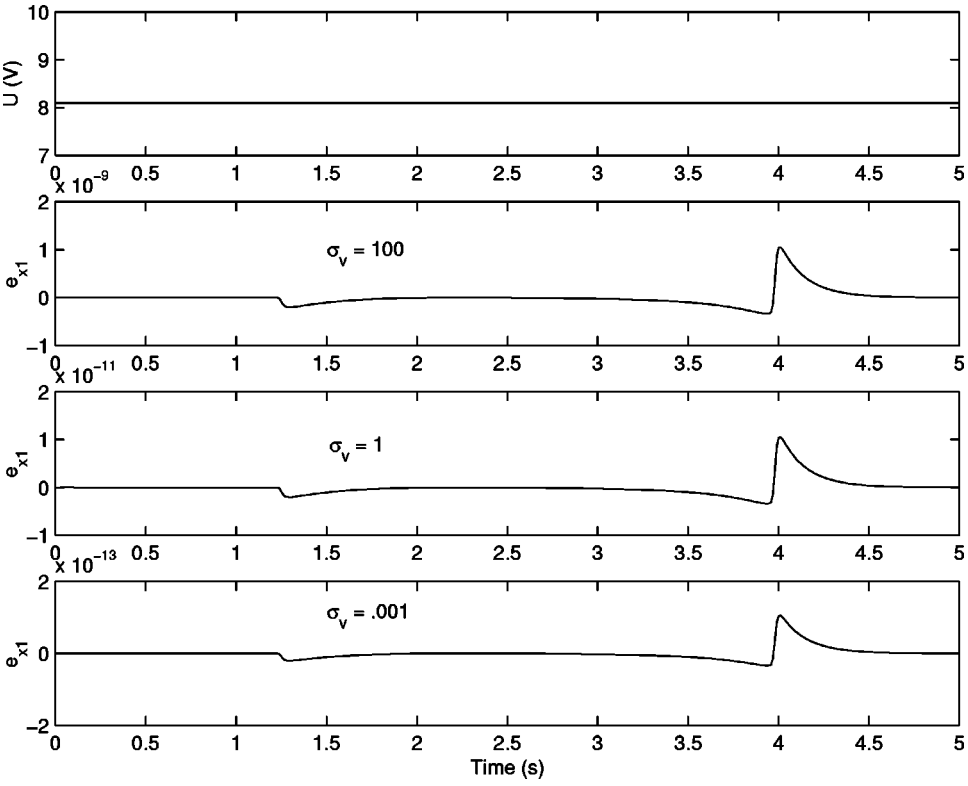

Fig. 5 The effect of the measurement noise covariance σ_v on the arm angular position prediction error of the extended Kalman filter, σ_w=1

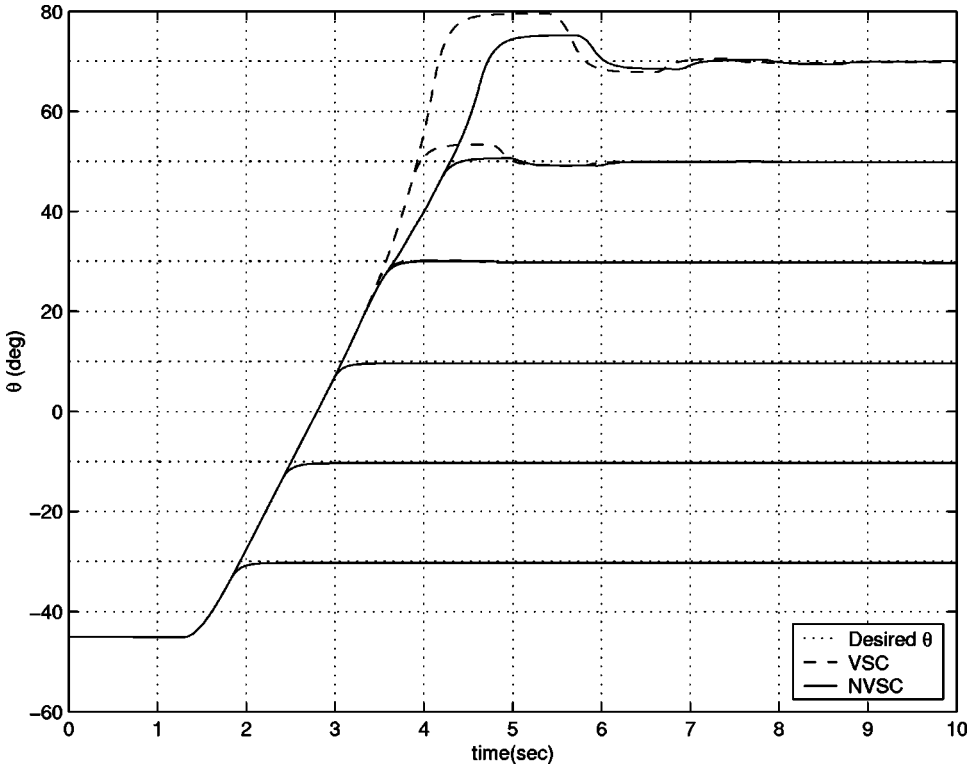

Fig. 6 Comparing the performance of the new VSC (based on position and velocity feedbacks and an EKF estimator) with the performance of the previous VSC (based on position and *v* velocity feedbacks only)

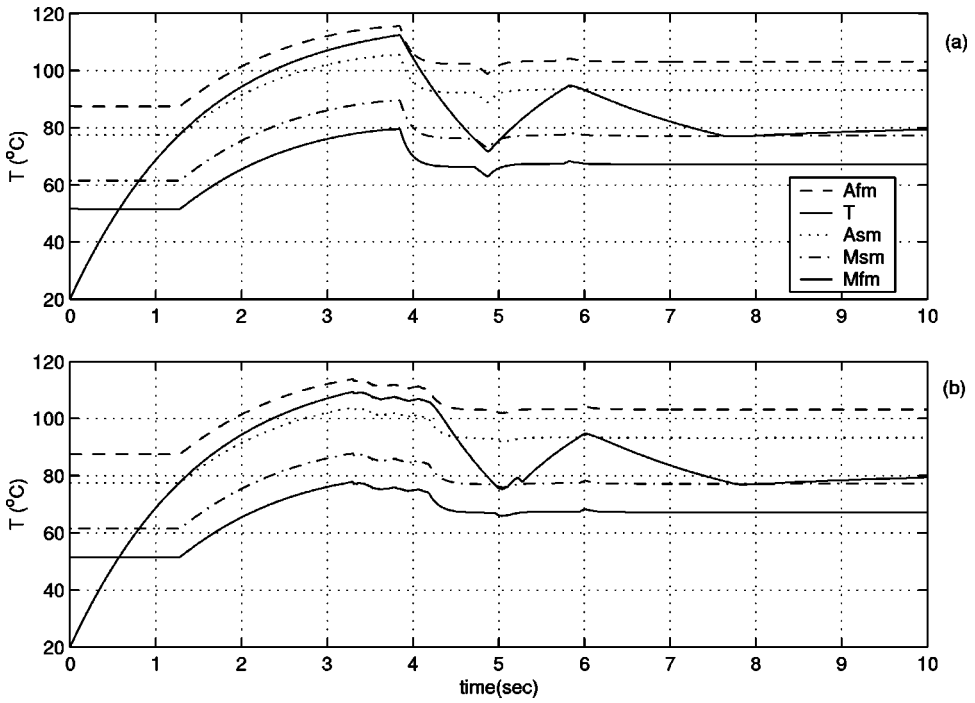

Fig. 7 The transformations and SMA wire temperatures for (*a*) previous VSC (based on position and velocity feedbacks only) and (*b*) new VSC (based on position and velocity feedbacks and an EKF estimator); desired angular position θ_d=50°

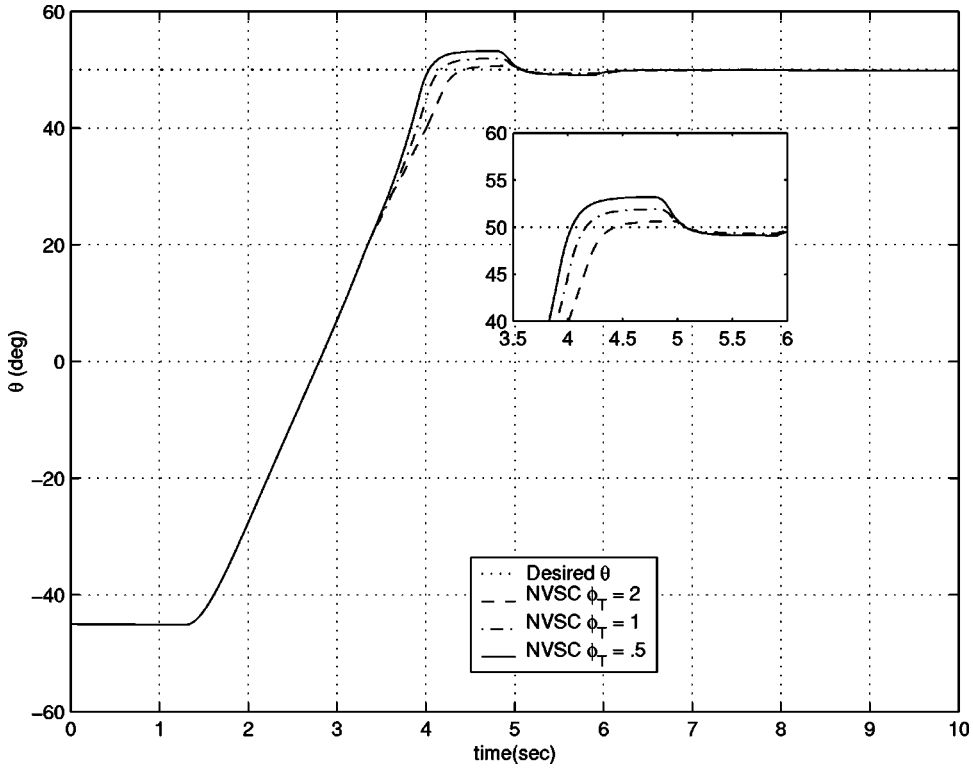

Fig. 8 The effect of the temperature boundary thickness ϕ_T°C/s on the overshoot minimization performance of the NVSC, for θ_d=50°

factory results have been shown in terms of the filter estimating a state vector that closely matches the state vector generated by a nonlinear model of the system. Since the model had been previously verified against experimental data and the filter is designed based on this model, it is expected that the filter can accurately estimate the state vector of the SMA actuated arm. Model uncertainties can degrade the estimation. However, these uncertainties can be included in the filter and therefore reduce the adverse effect. It is also shown that the filter performance is sensitive to measurement and process noise and sampling time but not to error in the state variable initial conditions.

In our previous work [13], we had shown both by simulation and experiments that a simple VSC has a robust performance for regulation, tracking, and disturbance rejection. However, overshoot can still occur when large rotations are required since the arm goes beyond the maximum-stress-position and therefore the transformation temperatures decrease. In this work, EKF is used to estimate the SMA wire stress and temperature and incorporate them into a modified VSC system. The new controller is shown to reduce or avoid overshoot while enjoying the desirable characteristics of our original controller.

References

[1] Kalman, R. E., 1960, "A New Approach to Linear Filtering and Prediction Problems," ASME J. Basic Eng., **82**, pp. 35–45.

[2] Welch, G., and Gary, B., 2001, "An Introduction to the Kalman Filter," *SIGGRAPH 2001, Los Angeles, CA August 12–17, 2001.*

[3] Gourdeau, R., and Schwartz, H. M., 1993, "Adaptive Control of Robotic Manipulators Using an Extended Kalman Filter," J. Dyn. Syst., Meas., Control, **115**(1), 203–208.

[4] Lertpiriyasuwat, V., Berg, M. C., and Buffinton, K. W., 2000, "Extended Kalman Filtering Applied to a Two-axis Robotic Arm with Flexible Links," Int. J. Robot. Res., **19**(3), pp. 254–270.

[5] Lin, J., and Lewis, F. L., 1993, "Improved Measurement/Estimation Technique for Flexible Link Robot Arm Control," *Proceedings of the 32nd Conference on Decision and Control, San Antonio, TX*, Vol. 1, pp. 627–632.

[6] Necsulescu, D., and Jassemi-Zargani, R., 2001, "Extended kalman filter based sensor fusion for operational space control of a robot arm," *Proceedings of IEEE Instrumentation and Measurement Technology Conference*, Vol. 2, pp. 915–918.

[7] Timcenko, A., and Kircanski, N., 1992, "Control of Robots with Elastic Joints: Deterministic Observer and Kalman Filter Approach," *Proceedings of the IEEE International Conference on Robotics and Automation, Nice, France*, Vol. 1, pp. 722–727.

[8] Arai, S., Aramaki, K., and Yanagisawa, Y., 1994, "Continuous System Modeling of Shape Memory Alloy (SMA) for Control Analysis," *Proceedings of the 5th IEEE International Symposium on Micro Machine and Human Science*, pp. 97–99.

[9] Carpenter, B., Head, R. J., and Gehling, R., 1995, "Shape Memory-actuated Gimbal," *Proceedings of SPIE—The International Society of Optical Engineering, San Diego, CA*, Vol. 2447, pp. 91–101.

[10] Gharaybeh, M. A., and Burdea, G. C., 1995, "Investigation of a Shape Memory Alloy Actuator Force-Feedback Masters," Adv. Rob., **9**(3), pp. 317–329.

[11] Hashimoto, M., Takeda, M., Sagawa, H., and Chiba, I., 1985, "Application of Shape Memory Alloy to Robotic Actuators," J. Rob. Syst., **2**(1), pp. 3–25.

[12] Arai, S., Aramaki, K., and Yanagisawa, Y., 1995, "Feedback Linearization of SMA (Shape Memory Alloy)," *Proceedings of the 34th SICE Annual Conference*, pp. 519–522.

[13] Elahinia, M. H., and Ashrafiuon, H., 2002, "Nonlinear Control of a Shape Memory Alloy Actuated Manipulator," ASME J. Vibr. Acoust., **124**, pp. 566–575.

[14] Grant, D., and Hayward, V., 2000, "Constrained Force Control of Shape Memory Alloy Actuators," *Proceedings of the IEEE International Conference on Robotics and Automation*, pp. 1314–1320.

[15] Nakazato, T., Kato, Y., and Masuda, T., 1993, "Control of Push-pull-type Shape Memory Alloy Actuators by Fuzzy Reasoning," Trans. Jpn. Soc. Mech. Eng., Ser. C, **59**(568), pp. 226–232.

[16] Liang, C., and Rogers, C. A., 1990, "One-dimensional Thermomechanical Constitutive Relations for Shape Memory Materials," J. Intell. Mater. Syst. Struct., **1**(2), pp. 207–234.

[17] Shahin, A. R., Meckl, P. H., Jones, J. D., and Thrasher, M. A., 1994, "Enhanced Cooling of Shape Memory Alloy Wires Using Semiconductor Heat Pump Modules," J. Intell. Mater. Syst. Struct., **5**(1), pp. 95–104.

[18] Tanaka, Y., 1986, "A Thermomechanical Sketch of Shape Memory Effect: One-dimensional Tensile Behavior," Res Mechanica, the International Journal of Structural Machines and Materials Science, **18**(1), pp. 251–263.

[19] Elahinia, M. H., Ahmadian, M., and Ashrafiuon, H., 2004, "Design of Kalman Filter for Rotary Shape Memory Alloy Actuators," Journal of Smart Materials and Structures, **13**(4), pp. 691–697.